

Comparative study of one-dimensional NiCo alloy nanostructures assembled by in situ and ex situ applied magnetic fields

WU Ming-zai(吴明在)^{1,2}, QUAN Gui-ying(全桂英)², LIU Yan-mei(刘艳美)²,
MA Yong-qing(马永青)², DAI Peng(戴 鹏)², ZHANG Li-de(张立德)¹

1. Key Laboratory of Materials Physics, Institute of Solid State Physics, Chinese Academy of Sciences, Hefei 230031, China;

2. Key Laboratory of Opto-electronic Information Acquisition and Manipulation of Ministry of Education, Anhui University, Hefei 230039, China

Received 10 August 2009; accepted 15 September 2009

Abstract: For the study of magnetic field-assisted assembly behavior, one-dimensional (1D) NiCo alloy nanostructures were solvothermally obtained at 180 °C under an in situ magnetic field (the magnetic field as applied during the chemical reduction) and ex situ field (after the chemical reduction was finished). Microscopic morphology and magnetic properties differences were investigated using scanning electronic microscope (SEM) and vibrating sample magnetometer (VSM) for these products. Magnetic measurement results show that 1D ordered microstructures under in situ magnetic field possess higher saturation magnetization M_s , remnant magnetization M_r , coercivity H_c and reduced magnetization M_r/M_s than 1D ordered microstructures under ex situ field, and the four magnetic parameters of the two ordered microstructures are much higher than those randomly distributed alloy particles prepared in the absence of external magnetic field.

Key words: NiCo alloy; assembly; magnetic field

1 Introduction

Traditionally, magnetic field has long been regarded as a method for studying magnetic properties of materials[1–3]. Until recently, much attention has been attracted for the possibility that magnetic fields could be used to influence chemical reactions, just like the off-used parameters, temperature and pressure[4]. In the past 5 years, the application of magnetic field has been explored in the hydrothermal processing[5–10]. Polycrystalline Co and Ni microwires were formed by the self-assembly of Co and Ni nanocrystallites under a 0.25 T external magnetic field[5–7]. Single crystalline Fe_3O_4 nanowires were obtained under the induction of an applied external field[8]. In addition to the well-known wire-like micro/nano structures, the legume-like structure of cobalt nanoparticles and the chain-like structure of magnetite nanoparticles are newly added

[9–10]. Despite these achievements, all of these researches were focused on the in situ application of magnetic field. Little attention has been paid to the detailed difference between the in situ application of filed and the ex situ magnetic field application (postsynthesis magnetic field application).

Ni-Co binary alloy possesses great applications in microelectromechanical systems (MEMS) and aeronautics for its high hardness and excellent soft magnetic performances[11], all of which are dependent on particle morphologies, texture and magnetic properties of the alloy. In this work, Ni-Co alloy was chosen for the comparative study of the morphology and magnetic properties difference between in situ and ex situ application of magnetic field.

2 Experimental

For the present experiment, all the reagents are

Foundation item: Project(50901074) supported by the National Natural Science Foundation of China; Project(20080430778) supported by China Postdoctoral Science Foundation; Project(2008jq1002) supported by Young Teacher Natural Science Foundation of Anhui Province, China

Corresponding author: ZHANG Li-de; Tel: +86-15955127125; E-mail: ldzhang@issp.ac.cn

DOI: 10.1016/S1003-6326(09)60070-4

of analytical grade and were used as received. 2 mmol cobalt acetyl acetonate (0.520 g), 2 mmol nickel acetyl acetonate (0.514 g), 20 mmol urea (1.2 g) and 1.0 g PVP were dissolved in ethylene diamine (70 mL). After being vigorously stirred for 15 min, 10.0 mL hydrazine was dropwise added into the above mixture solution. Then, the tawny solution was transferred into two Teflon-lined stainless steel autoclaves with 60 mL capacity, respectively (one without external magnetic field, the other with 0.18 T magnet made of NdFeB). Both of the autoclaves were closed tightly to perform solvothermal processes at 180 °C for 12 h. After the reaction was completed, the resulting black solid powder was washed with alcohol and distilled water three times, respectively. Then the products were dried in air at 50 °C. The as-obtained samples were labeled as ZF and AF18, indexing to the samples with zero magnetic field and with 0.18 T one respectively. The same reactions were performed for the case of 0.34 T field, which yielded sample AF34. AF18P and AF34P were used to index the postsynthesis magnetic assembly with 0.18 T and 0.34 T field, respectively, which could be obtained by scrapping the aligned ZF particles dispersed in the ethanol on the wafer. These samples were characterized by X-ray powder diffraction (XRD) using an 18 kW advanced X-ray diffractometer with Cu K α radiation ($\lambda=1.540\ 56\ \text{\AA}$), field emission scanning electron microscope (FESEM, FEI Sirion 200). Magnetic hysteresis loops were measured on a vibrating sample magnetometer (VSM, BHV-55) at room temperature.

3 Results and discussion

The phases of the samples ZF, AF18, AF34 were determined by XRD with the patterns shown in Fig.1. All peaks can be indexed to face-centered cubic structure.

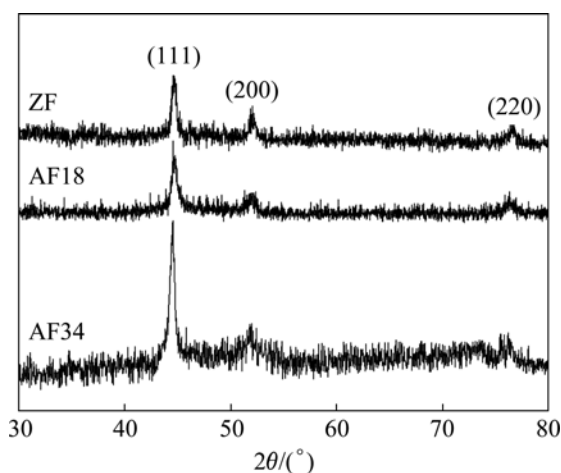


Fig.1 XRD patterns of samples ZF, AF18 and AF34

The substitution of Ni and Co atoms in the alloys results in the chemical disorder and poor crystallinity. The crystallite size of ZF (21 nm) is smaller than that of AF18 (33) or AF34 (42 nm), calculated by Scherrer's equation from the full width at half-maximum of (111) reflection, which reveals the fact that the application of magnetic fields can enhance the crystallite size. Remarkably, the intensity ratio of (111) peak to (200) peak increases with the increase of magnetic field strength, indicating a preferential orientation of alloy grains in the 1D nanostructures, and becomes more distinct when the magnetic field is increased. These results suggest that the nucleation and growth of crystallites can be influenced by magnetic fields.

The field emission scanning electron microscopy (FESEM) images of samples ZF, AF18, AF18P, AF34 and AF34P are shown in Fig.2 and Fig.3. With no field applied, spherical particles with an average diameter of about 1 μm distribute randomly, shown in Fig.2(a). The difference between the observed size and Scherrer's calculation reveals that the spherical particles are polycrystalline. Interestingly, 1D microstructures were obtained when magnetic fields were applied. Figs.2(b–d) show the morphologies of samples AF34 and AF34P, which clearly reveals the differences between the in situ magnetic field and the ex situ one in terms of microscopic morphology of the products. The panoramic image of sample AF34 in Fig.2(b) is composed of bundles of microstructures with average length of 200 μm . Although AF34P also possesses shape of bundles of microstructures, there are microscopic morphology differences from AF34. Figs.2(c) and (d) show the enlarged bundles of AF34 and AF34P, respectively. Compared with AF34, it is concluded that AF34P is made of one-particle chain, with chainlike structures and is not as uniform and continuous as wire-like AF34. In fact, the constituent units of the wire-like AF34 are linked so tightly that we cannot differentiate them. This observation further reveals that the 0.34 T magnetic field can exert much influence on the nucleation and growth of the magnetic particles during the hydrothermal reduction instead of a simple assembly. Both AF34 and AF34P microstructures are too large to be characterized by high-resolution transmission electron microscope (HRTEM), and further investigations are under way.

Fig.3(a) shows a lower magnetization SEM image of sample AF18, which reveals many loose wire-like nanostructures with over 30 μm in length and about 800 nm in diameter, interconnected with each other. More details about these wires can be found in Fig.3(b). Evidently, the single wire in Fig.3(b) is seamlessly linked

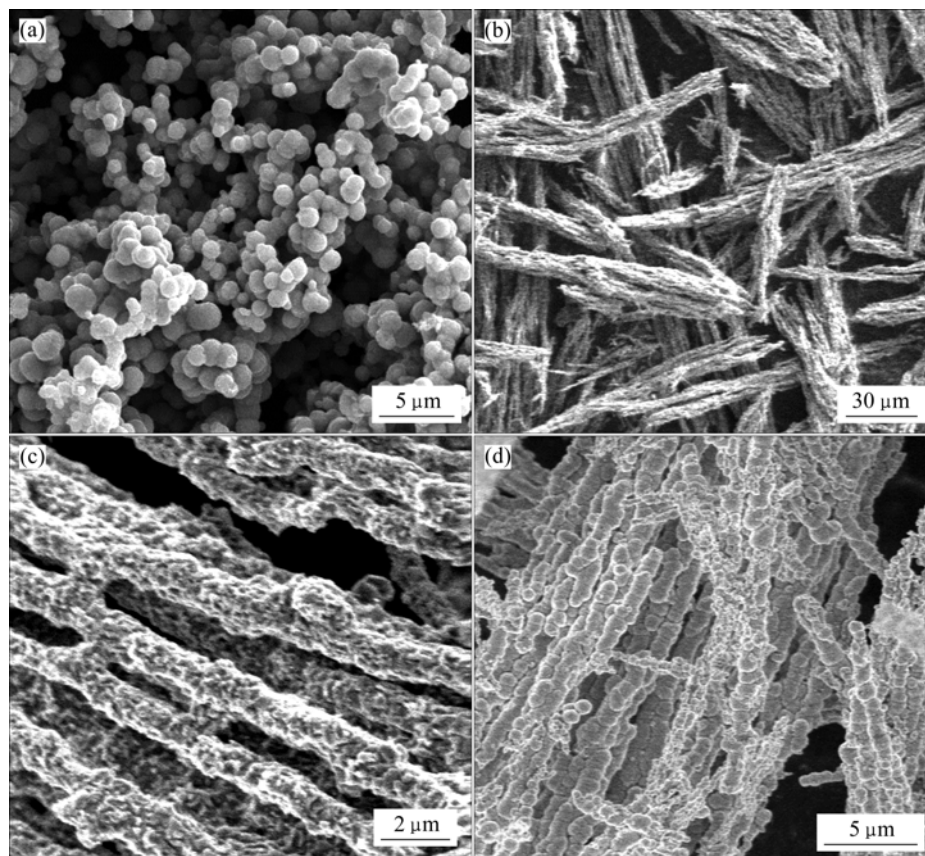


Fig.2 SEM micrographs of products prepared under different conditions: (a) ZF sample; (b) Lower magnification SEM image of AF34; (c) Higher magnification SEM image of AF34; (d) AF34P

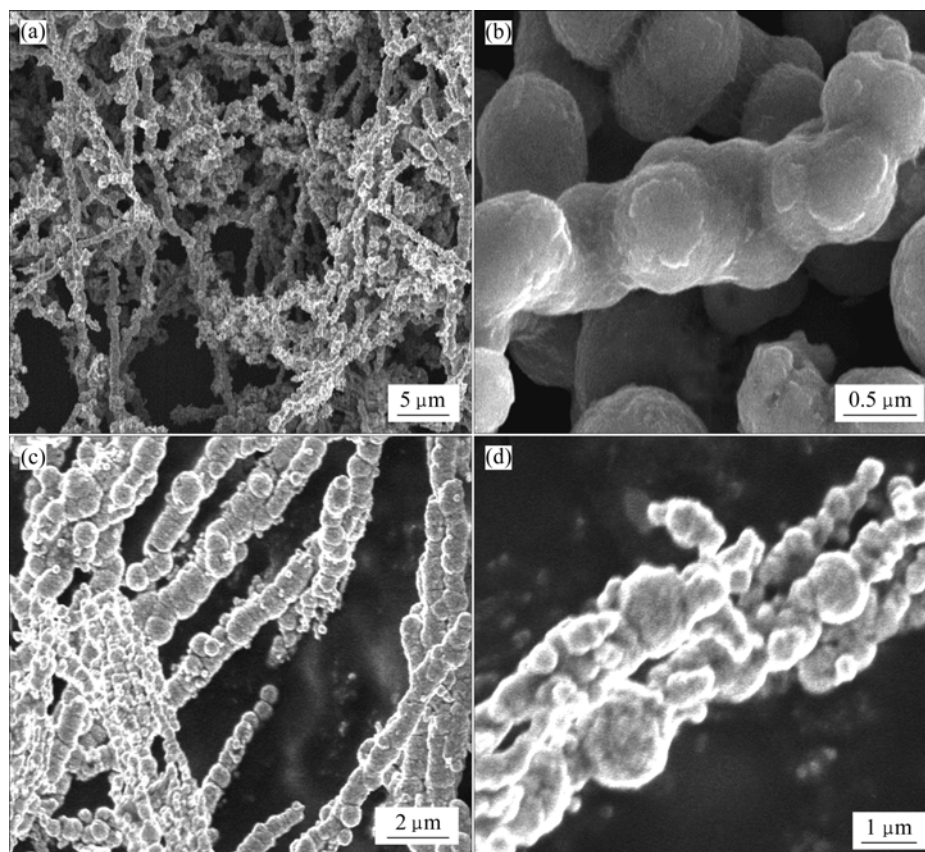


Fig.3 SEM micrographs of products prepared under different conditions: (a) Lower magnification SEM image of AF18; (b) Higher magnification SEM image of AF18; (c) Lower magnification SEM image of AF18P; (d) Chain-like particle of AF34P

by these nearly spherical particles. These building particles keep the spherical shape, which is a little different from that of AF34. The reason should be from the difference of magnetic field intensity. The stronger the applied magnetic field is, the larger the changes of the particles morphologies are. Comparatively, Figs.3(c) and (d) show the images of AF18P. On the whole, AF18P is composed of chain-like microstructures, similar to that of AF34P. However, these chains are not aligned as orderly as those of AF34P (Fig.3(c)). In addition, some chains are very rough, accompanied with some smaller particles, which can no longer be called one-particle chain (Fig.3(d)). The above observation can be explained based on the reduced alignment and the reduced interaction between particles and applied magnetic field.

The magnetic properties of materials are believed to be highly dependent on the sample morphology, crystallinity, magnetization direction, etc[11]. Hence, the ferromagnetic properties of 1D microstructures of AF34, AF34P, AF18 and AF18P are supposed to be remarkably different from those of disordered ZF. Fig.4 shows $M-H$ hysteresis loops of the products measured at room temperature. The inset is the enlarged plots of boxed area in Fig.4. The main magnetic parameters including saturation magnetization M_s , remnant magnetization M_r , reduced magnetization M_r/M_s and coercive field H_c are listed in Table 1.

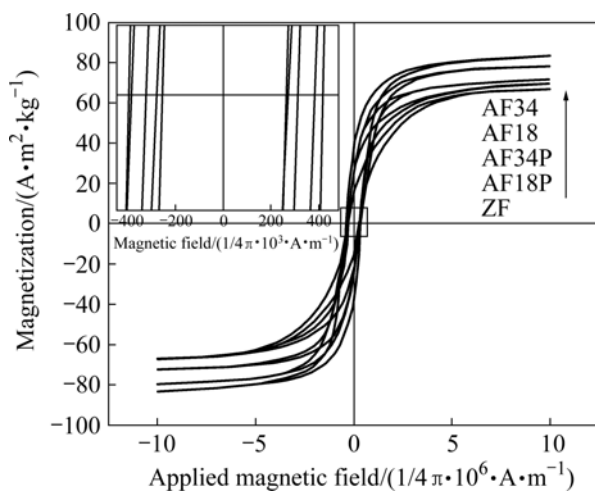


Fig.4 Field-dependent magnetization of samples ZF, AF18P, AF34P, AF18 and AF34 measured at 300 K in applied magnetic field

Compared with M_s of the ZF sample ($66.5 \text{ A} \cdot \text{m}^2/\text{kg}$), all samples of the in situ magnetic field and the ex situ one possess enhanced M_s , especially for the AF34 ($82.9 \text{ A} \cdot \text{m}^2/\text{kg}$). Noticeably, in situ magnetic field exerts much more distinct effect than ex situ one in terms of the

Table 1 Magnetic parameters M_s , M_r , M_r/M_s , H_c of samples ZF, AF18P, AF34P, AF18 and AF34 obtained by VSM measurement at room temperature

Sample	Parameter			
	$M_s/$ ($\text{A} \cdot \text{m}^2 \cdot \text{kg}^{-1}$)	$M_r/$ ($\text{A} \cdot \text{m}^2 \cdot \text{kg}^{-1}$)	M_r/M_s	$H_c/$ ($1/4\pi \cdot 10^3 \cdot \text{A} \cdot \text{m}^{-1}$)
ZF	66.5	14.1	0.21	270
AF18P	69.5	23.2	0.33	268
AF34P	70.8	25.2	0.35	313
AF18	78.1	26.5	0.34	384
AF34	82.9	36.3	0.44	418

enhancement of M_s and H_c values, which maybe result from the effect of in situ magnetic field on the nucleation and growth of particles. Consistently, the values of reduced remanence (M_r/M_s) of samples AF18 and AF34 are larger than those of the samples ZF, AF18P or AF34P. Furthermore, with the increase of the magnetic field intensity, the differences between the sample ZF and samples of AF series are enhanced, which holds for all the four magnetic parameters. As discussed above, the nucleation and growth of alloy particles along the magnetic force line determine the 1D microstructures formation. Therefore, it is expected that a weak magnetic field can be developed as an important tool to control the structure and properties of materials, especially magnetic materials. The present study reveals that the structure and morphology can be artificially tuned by using both the in situ magnetic field and the ex situ one.

4 Conclusions

1) In situ magnetic field and ex situ field were successfully applied for the preparation of 1D NiCo alloy nanostructures.

2) Based on the XRD analysis and SEM images observation, it is concluded that the in situ magnetic field can synchronously influence both the nucleation and the parallel growth of particles, while the ex situ applied field only assembles the particles into chain-like microstructures.

3) Magnetic measurements reveal that in situ magnetic field exerts much more distinct effect than ex situ one in terms of the enhancement of M_s values and H_c values, which are believed to result from the effect of in situ magnetic field on the nucleation and growth of particles. It is suggested that the reasonable choice of in situ magnetic field and ex situ one can serve as promising method for the preparation of novel

nanostructures and modulation of magnetic properties.

References

- [1] LEVY F, SHEIKIN I, GRENIER B, HUXLEY A D. Magnetic field-induced superconductivity in the ferromagnet UrhGe [J]. *Science*, 2005, 309: 1343–1346.
- [2] RABANI E, REICHMAN D R, GEISSLER P L, BRUS L E. Drying-mediated self-assembly of nanoparticles [J]. *Nature*, 2003, 426: 271–274.
- [3] JANKOVIC L, GOURNIS D, TRIKALITIS P N, ARFAOUI I, CRENT, RUDOLF P, SAGE M H, PALSTRA T T M, KOOI B, HOSSON J D, KARAKASSIDES M A, DIMOS K, MOUKARIKA A, BAKAS T. Carbon nanotubes encapsulating superconducting single-crystalline tin nanowires [J]. *Nano Lett*, 2006, 6: 1131–1135.
- [4] STASS D V, WOODWARD J R, TIMMEL C R, HORE P J, MCLAUCHLAN K A. Radiofrequency magnetic field effects on chemical reaction yields [J]. *Chem Phys Lett*, 2000, 329: 15–22.
- [5] NIU H L, CHEN Q W, ZHU H F, LIN Y S, ZHANG X. Magnetic field-induced growth and self-assembly of cobalt nanocrystallites [J]. *J Mater Chem*, 2003, 13: 1803–1805.
- [6] NIU H L, CHEN Q W, NING M, JIA Y S, WANG X J. Synthesis and one-dimensional self-assembly of acicular nickel nanocrystallites under magnetic fields [J]. *J Phys Chem B*, 2004, 108: 3996–3999.
- [7] SUN L X, CHEN Q W, TANG Y, XIONG Y. Formation of one-dimensional nickel wires by chemical reduction of nickel ions under magnetic fields [J]. *Chem Commun*, 2007, 27: 2844–2846.
- [8] WANG J, CHEN Q W, ZENG C, HOU B Y. Magnetic-field-induced growth of single-crystalline Fe_3O_4 nanowires [J]. *Adv Mater*, 2004, 16: 137–140.
- [9] XIONG Y, CHEN Q W, TAO N, YE J, TANG Y, FENG J S, GU X Y. The formation of legume-like structures of Co nanoparticles through a polymer-assisted magnetic-field-induced assembly [J]. *Nanotechnology*, 2007, 18: 345301–345305.
- [10] WU M Z, XIONG Y, JIA Y S, NIU H L, QI H P, YE J, CHEN Q W. Magnetic field-assisted hydrothermal growth of chain-like nanostructure of magnetite [J]. *Chem Phys Lett*, 2005, 401: 374–379.
- [11] LIU Z P, LI S, YANG Y, PENG S, HU Z K, QIAN Y T. Complex-surfactant-assisted hydrothermal route to ferromagnetic nickel nanobelts [J]. *Adv Mater*, 2003, 15: 1946–1948.

(Edited by YANG Hua)